Cytotherapy 23 (2021) 25–36

Contents lists available at ScienceDirect

CYTOTHERAPY

journal homepage: www.isct-cytotherapy.org

FULL-LENGTH ARTICLE

Basic Research

Indirect co-culture of lung carcinoma cells with hyperthermia-treated mesenchymal stem cells influences tumor spheroid growth in a collagen-based 3-dimensional microfluidic model

Nandini Dhiman[1,2], Nadin Shagaghi[1], Mrinal Bhave[1], Huseyin Sumer[1], Peter Kingshott[1,3,*], Subha Narayan Rath[2,**]

[1] Department of Chemistry and Biotechnology, Faculty of Science, Engineering and Technology, Swinburne University of Technology, Hawthorn, Australia
[2] Regenerative Medicine and Stem Cell Laboratory, Department of Biomedical Engineering, Indian Institute of Technology Hyderabad, Medak, India
[3] ARC Training Centre in Surface Engineering for Advanced Materials, School of Engineering, Swinburne University of Technology, Hawthorn, Australia

ARTICLE INFO

Article History:
Received 30 May 2020
Accepted 2 July 2020

Key Words:
mesenchymal stem cells
microfluidic cancer model
MSC-conditioned medium
lung tumor spheroids
3D cell culture

ABSTRACT

Background: Mesenchymal stem cells (MSCs) have paradoxically been reported to exert either pro- or anti-tumor effects *in vitro*. Hyperthermia, in combination with chemotherapy, has tumor-inhibiting effects; however, its role, together with MSCs, so far is not well understood. Furthermore, a lot of research is conducted using conventional 2-dimensional *in vitro* models that do not mimic the actual tumor microenvironment.
Aim: In light of this fact, an indirect method of co-culturing human amniotic membrane-derived MSCs (AMMSCs) with collagen-encapsulated human lung carcinoma cells (A549) was performed using a 3-dimensional (3D) tumor-on-chip device.
Methods: The conditioned medium of AMMSCs (AMMSC-CM) or heat-treated AMMSCs (heat-AMMSC-CM) was utilized to create indirect co-culture conditions. Tumor spheroid growth characterization, immunocytochemistry and cytotoxicity assays, and anti-cancer peptide (P1) screening were performed to determine the effects of the conditioned medium.
Results: The A549 cells cultured inside the 3D microfluidic chip developed into multicellular tumor spheroids over five days of culture. The AMMSC-CM, contrary to previous reports claiming its tumor-inhibiting potential, led to significant proliferation of tumor spheroids. Heat-AMMSC-CM led to reductions in both spheroid diameter and cell proliferation. The medium containing the P1 peptide was found to be the least cytotoxic to tumor spheroids in co-culture compared with the monoculture and heat-co-culture groups.
Conclusions: Hyperthermia, in combination with the anticancer peptide, exhibited highest cytotoxic effects. This study highlights the growing importance of 3D microfluidic tumor models for testing stem-cell-based and other anti-cancer therapies.

Introduction

Mesenchymal stem cells (MSCs) have the unique ability to self-renew indefinitely and differentiate into multiple lineages, such as fat, bone, muscle and cartilage [1]. In addition, MSCs have a distinctive property of homing, wherein they migrate to sites of injury and tumor microenvironments in response to specific signaling factors [2,3]. This property of MSCs has brought an exciting opportunity to use them for cancer cytotherapy [4]. MSCs can be injected systemically to deliver therapeutics after reaching the tumor site, thereby providing targeted drug delivery without affecting healthy cells in the vicinity [5]. Although genetically modified MSCs have shown some positive results in this regard in *ex vivo* and animal models [6], non-modified MSCs have shown conflicting therapeutic results *in vivo* and *in vitro* [4].

MSCs were initially isolated from bone marrow; however, they can now be isolated from other tissues, such as adipose, umbilical cord (Wharton's jelly) and amniotic membrane tissue, as well as umbilical cord blood [1]. Recent developments have shown that MSCs obtained

* Correspondence: Prof. Peter Kingshott (PhD), Department of Chemistry and Biotechnology, Faculty of Science, Engineering and Technology, Swinburne University of Technology, Hawthorn, Victoria 3122, Australia.
** Correspondence: Dr. Subha Narayan Rath (MBBS, MMST, PhD), Regenerative Medicine and Stem Cell Laboratory, Department of Biomedical Engineering, Indian Institute of Technology Hyderabad, Kandi, Sangareddy, Medak 502 285, Telangana, India.
E-mail addresses: pkingshott@swin.edu.au (P. Kingshott), subharath@bme.iith.ac.in (S.N. Rath).

https://doi.org/10.1016/j.jcyt.2020.07.004
1465-3249/

from different sources can have both pro-tumorigenic and anti-tumorigenic effects [4]. For example, MSCs derived from bone marrow and adipose tissue have mostly demonstrated tumor-enhancing effects, whereas MSCs from umbilical sources have shown mainly tumor-suppressing effects [4]. Amniotic membrane-derived MSCs (AMMSCs) have also shown anti-tumor effects, although uncertainty still exists in the current literature regarding this potential [7]. Furthermore, results are inconsistent between the different cancer cell lines and different tumor model types used in many of the reports. These observations motivate further exploration of the role of MSCs in cancer growth. Stem cell-based cancer therapies involve choosing cells that have potential anti-tumor effects and can home to tumor sites to deliver chemotherapeutic drugs at the cancer site to achieve selective cytotoxic results against cancer cells. Before this can be considered a novel therapeutic regime, however, a lot of research and optimization needs to be done concerning the potential effects of MSCs in cancer treatment.

Given that cancers are highly heterogeneous and evolving in nature, combinatorial and targeted therapies would definitely pave the way for the discovery of future cancer treatments [8]. Hyperthermia is one such cancer therapy technique that involves localized heat treatment at a tumor tissue site at temperatures between 42°C and 46°C for 45–60 min [9,10]. Hyperthermia as a combination treatment, along with chemotherapy, leads to an increase in blood flow in the tumor mass that further increases the concentration of the drugs, which is one of the reasons behind its tumor-inhibiting effects [11–13]. However, research on its effects on tumor stromal cells has been limited in the past. Since MSCs are significant constituents of the tumor stroma, it is essential to also study the impact of hyperthermia on these cells.

One of the major limiting factors in the previous literature about cancer cells is that in the majority of the studies, the cells were cultured on conventional 2-dimensional (2D) culture well plates [4,14,15]. These traditional methods have significant disadvantages: cells in monolayer cultures do not mimic tumor cells *in vivo*, they have poor cell morphology and there is loss of secreted growth factors in the large volume of culture medium [16,17]. The tumors *in vivo* are 3-dimensional (3D) in nature (multicellular spheroids) and are composed of cancer cells, along with other cell types, adhered to the 3D matrix, and cell-matrix interactions constantly regulate the tumor microenvironment. An advanced approach that utilizes microfluidic chips for cancer cell culture in a 3D hydrogel is showing great promise at overcoming some of the limitations of 2D *in vitro* cell cultures [14,15,17].

Microfluidic devices have gained considerable attention with regard to cell biology research [18]. These devices manipulate fluids at the micrometer to sub-micrometer range ($0.1\text{-}1 \times 10^{-6}$ m). The ruling physical principles at the microscale are radically different from those operating at the macroscale. For example, the presence of laminar flow and diffusion dominates over convection; more interestingly, these are the physical parameters that also regulate biochemical processes in tissue/tumor microenvironments. Other advantages microfluidic technology provides are precise handling of cells and hydrogels, spatiotemporal distribution of cells and biomolecules and design of co-cultures, such as use of endothelial cells for mimicking the vasculature [18,19]. The most significant advantage of this technology lies in cost-savings, as the requirement for cells, media and drugs is low, which means this approach becomes more cost-effective when the need for large numbers of experimental samples increases, such as in drug screening.

Here we have attempted an indirect co-culture of AMMSCs and cancer cells and also tested the effects of hyperthermia-treated AMMSCs in combination with an anti-cancer peptide (ACP) drug on A549 lung cancer cells embedded in collagen hydrogel inside a 3D microfluidic device. The indirect co-culture was achieved using the conditioned medium of AMMSCs (AMMSC-CM) or heat-treated AMMSCs (heat-AMMSC-CM). The conditioned medium, also known as the secretome of MSCs, has gained popularity in testing for cancer therapeutics since the paracrine factors released by MSCs are the main driving force behind the therapeutic abilities of MSCs [20,21]. We hypothesized that AMMSCs would exert either pro- or anti-tumor effects and that hyperthermia would exert an anti-tumor effect in the indirect co-culture system with cancer cells on-chip. To the best of our knowledge, this is the first time that co-culture (indirect or direct) of cancer cells with AMMSCs has been performed in a 3D microfluidic cancer model.

Methods

Microfluidic device fabrication

The SU-8 100 (MicroChem, Texas, USA) photoresist-based UV photolithography was used to generate a silicon-SU-8 (Si-SU-8) master that was then replica-molded to create polydimethylsiloxane (PDMS) (Sylgard 184; Dow Chemical Pty Ltd, Victoria, Australia) microfluidic chips, as described in the authors' previous work [22]. Briefly, after overnight silanization of the Si-SU-8 master using trichloro (1h,1h,2h,2h-perfluorooctyl)silane (Sigma- Aldrich, New South Wales, Australia), PDMS at a ratio of 1:10 was mixed, degassed and poured over the SI-SU-8 master and cured at 70°C for 6 h. The cured PDMS was then peeled off carefully, punched at the inlets/outlets, cleaned and dried. The PDMS replicas were bonded to glass coverslips using oxygen plasma treatment (Tergeo plasma cleaner; PIE Scientific LLC, Union City, CA, USA) to form closed microchannels. The devices were then coated with 2 mg/mL^{-1} polydopamine (pH 8.5 in tris(hydroxymethyl)aminomethane hydrochloride buffer; Sigma- Aldrich, New South Wales, Australia), washed with distilled water and dried at 80°C for 24 h. The devices were sterilized with UV light for 40 min prior to cell culture.

Cell culture

Human AMMSCs (isolated primary cells utilized in previous studies [23,24]) were cultured in Dulbecco's Modified Eagle's Medium (Sigma-Aldrich, New South Wales, Australia) supplemented with 10% fetal bovine serum (Life Technologies Australia Pty Ltd, Victoria, Australia), 1.25% GlutaMAX (Life Technologies Australia Pty Ltd, Victoria, Australia) and 1% penicillin/streptomycin (Life Technologies Australia Pty Ltd, Victoria, Australia). The human lung adenocarcinoma cell line (A549) [25] was cultured in Dulbecco's Modified Eagle's Medium (Sigma-Aldrich) with 10% fetal bovine serum (Life Technologies), 1.25% GlutaMAX (Life Technologies Australia Pty Ltd, VIC, Australia) and 1% penicillin/streptomycin (Life Technologies Australia Pty Ltd, VIC, Australia). Both cell types were grown in 5% CO_2 at 37°C in a humidified incubator. The AMMSCs between passage numbers 3 and 5 were used in our experiments and were subcultured as described previously [26].

Hyperthermia treatment and preparation of conditioned medium

The human AMMSCs during the growth phase were subject to heat treatment (hyperthermia) in a humidified incubator. Two T-75 flasks containing AMMSCs were placed inside a humidified CO_2 incubator kept at 43°C for 45 min. The flasks were then transferred to a 37°C CO_2 incubator, and cells were cultured for another 24 h. The conditioned media from the heat-treated flasks were collected, filtered using 2-μm filters and stored at −20°C until further use. To obtain conditioned media without heat treatment, media were collected from the same number of AMMSCs (2 T-75 flasks) during the growth phase at the same time point as the heat-treated AMMSCs, and then filtered using 2-μm filters and stored at −20°C until further use.

Indirect 3D co-culture on-chip and experimental groups

The A549 cells were subcultured to obtain cell suspensions of 8×10^6cells/mL^{-1}. Next, 3 mg/mL^{-1} collagen gel solution (Life Technologies Australia Pty Ltd, Victoria, Australia) was diluted to 2 mg/mL^{-1} using sterile distilled water and 10X PBS and neutralized to pH 7.4 using 1N sodium hydroxide. The cell suspension was mixed with the collagen gel at a ratio of 1:10 to generate a final cell concentration of 0.5×10^6cells/mL^{-1}, as described previously [22]. Next, 10 μL of the cell-hydrogel mixture was injected into the gel channel of the microfluidic devices, introducing cells at a concentration of 5×10^3cells/mL^{-1}. The devices were kept inside a humidified 5% CO_2 incubator at 37°C for 30 min for gel polymerization, followed by medium insertion in the microchannels, and the devices were returned to the incubator for culture. For the indirect co-culture of A549 cells and AMMSCs, AMMSC-CM was applied to the microfluidic cultures (group renamed co-culture group) from day 0. Similarly, heat-AMMSC-CM was applied to the microfluidic cultures from day 0 (group renamed heat-co-culture group). The tumor microfluidic chips that were supplied with normal culture medium were named the monoculture group. The medium in the microfluidic devices was changed every 24 h during the duration of the experiment.

Image analysis for spheroid characterization

The diameter of the tumor spheroids in the 3 experimental groups was calculated from the bright-field images (Leica DM IL light microscope; Leica, Wetzlar, Germany) using the formula area = $\pi r^2$and circularity parameter of 0.8–1.0 with the help of ImageJ software [27]. Tumor cell aggregates with diameters >35 μm were considered spheroids [28,29]. The entire length of the microfluidic channel was considered a region of interest for calculating the size distribution of spheroids, the number of aggregates/spheroids and the average diameter (n = 20 images).

Immunocytochemistry and image analysis

Immunofluorescent staining was utilized to determine the expression of protein Ki-67 on day 5 of cell culture. Briefly, 4% paraformaldehyde was used to fix the 3D cultures in the microfluidic channels for 0.5 h, and the cells were then permeabilized using 0.1% Triton X-100 for 0.5 h. The cells were then treated overnight at a temperature of 4°C with 5% bovine serum albumin. In a dark room, the primary antibody against Ki-67 (Alexa Fluor 488-conjugated rabbit monoclonal antibody; Cell Signaling Technology, Queensland, Australia) was applied to the fixed cells overnight at a ratio of 1:200 at 4°C. The samples were then washed with pre-warmed 1X PBS and incubated with 4',6-diamidino-2-phenylindole (DAPI) (Sigma-Aldrich, St Louis, MO, USA) at a ratio of 1:10 for 3 h in the dark. Following this, imaging of the samples was performed using a confocal laser scanning microscope (FV3000; Olympus, Tokyo, Japan) after washing the samples 3 times with 1X PBS. Optical sections were taken at 3-μm intervals and stacked into a Z-projection. The power, intensity and offset settings were kept constant throughout the image acquisition. The fluorescence intensity of the final images was ascertained with the help of ImageJ software [27]. For quantitative comparison, the fluorescent intensity was normalized to the DAPI intensity.

Testing of ACP

The ACP used in this study was a cationic tryptophan-rich antimicrobial peptide called P1 (RKRWWRWWKWWKR-NH_2, where R is arginine, K is lysine and W is tryptophan). The synthesis and design of this particular peptide were described in detail in the authors' previous work, in which a charge-based mechanism attacked the cancer cells [22,30]. ACP was added to the complete culture medium (without penicillin/streptomycin) to prepare the final ACP media at 2 different test concentrations: 30 μM and 58 μM. Following a pre-warmed PBS wash, the prepared ACP media were added to the tumor spheroids in the microfluidic devices after 5 days in culture. The tumor spheroids in all groups were exposed to ACP for 72 h.

Cytotoxicity assay

To assess the effects of the indirect co-culture of AMMSCs on tumor spheroids, a cytotoxicity assay was performed after 5 days of cell culture on the chip. The LIVE/DEAD viability/cytotoxicity kit (Life Technologies Australia Pty Ltd, Victoria, Australia) was utilized according to the manufacturer's instructions to determine cell viability. After 72 h of ACP exposure to the cancer cells on-chip, the cytotoxicity assay was performed again to determine ACP cytotoxicity. Live cells were distinguished from dead cells by simultaneously staining the 3D culture using Calcein AM dye (green fluorescence), which acted on the intracellular esterase activity, and Ethidium Homodimer I dye (red fluorescence), which entered the cells that had lost the integrity of their plasma membrane. Previous studies, including the authors' own [22], have shown that both Calcein AM and Ethidium Homodimer I work very well with hydrogels, including collagen type 1, in both macroscale [31] and microscale cell cultures [28,29,32]. The channels were washed twice with pre-warmed PBS to remove background fluorescence and then imaged using a confocal laser scanning microscope. Optical sections were taken at 3-μm intervals and stacked into a Z-projection. The power, intensity and offset settings were kept constant throughout the image acquisition. Images were quantified using ImageJ software [27] by calculating the fluorescent area fractions for both live and dead cells.

Statistical analysis

All data were stated as mean ± standard deviation of 3 independent experiments. Statistical significance was tested using Student's *t*-test and 2-way analysis of variance, followed by Tukey's multiple comparisons test, using Prism 7.0 (GraphPad, San Diego, CA, USA). $P < 0.05$ and $P < 0.005$ were considered to be statistically significant.

Results and Discussion

Microfluidic device for 3D tumor cell culture

We designed a microfluidic chip to perform 3D cell culture of tumor cells as well as indirect co-culture with AMMSCs. The final microfluidic device consisted of 3 channels, each 1000-μm wide, as shown schematically in Figure 1A. The device also had 4 medium reservoirs (4-mm diameter) connecting the media channels and 2 reservoirs (1-mm diameter) connecting the central gel channel. The central channel was separated from the 2 media channels by an array of microposts that restricted the hydrogel within the channel and prevented leakage of the hydrogel during insertion and post-insertion before polymerization (Figure 1A). Figure 1B shows the respective gel and media channels in the fabricated device made out of PDMS. PDMS is highly biocompatible and gas permeable and therefore permits gaseous exchange (O_2 and CO_2) between the cell culture and environment. Furthermore, the bonded chips can be sterilized using UV owing to the transparency of PDMS to UV light.

The 3-channel device with these dimensions provided a straightforward and precise way to do 3D cell culture with considerably less reagent volume and cell numbers [33]. The media from the flanking channels diffused through the cell-laden hydrogel in the middle channel and sustained the supply of nutrients to the cells for at least

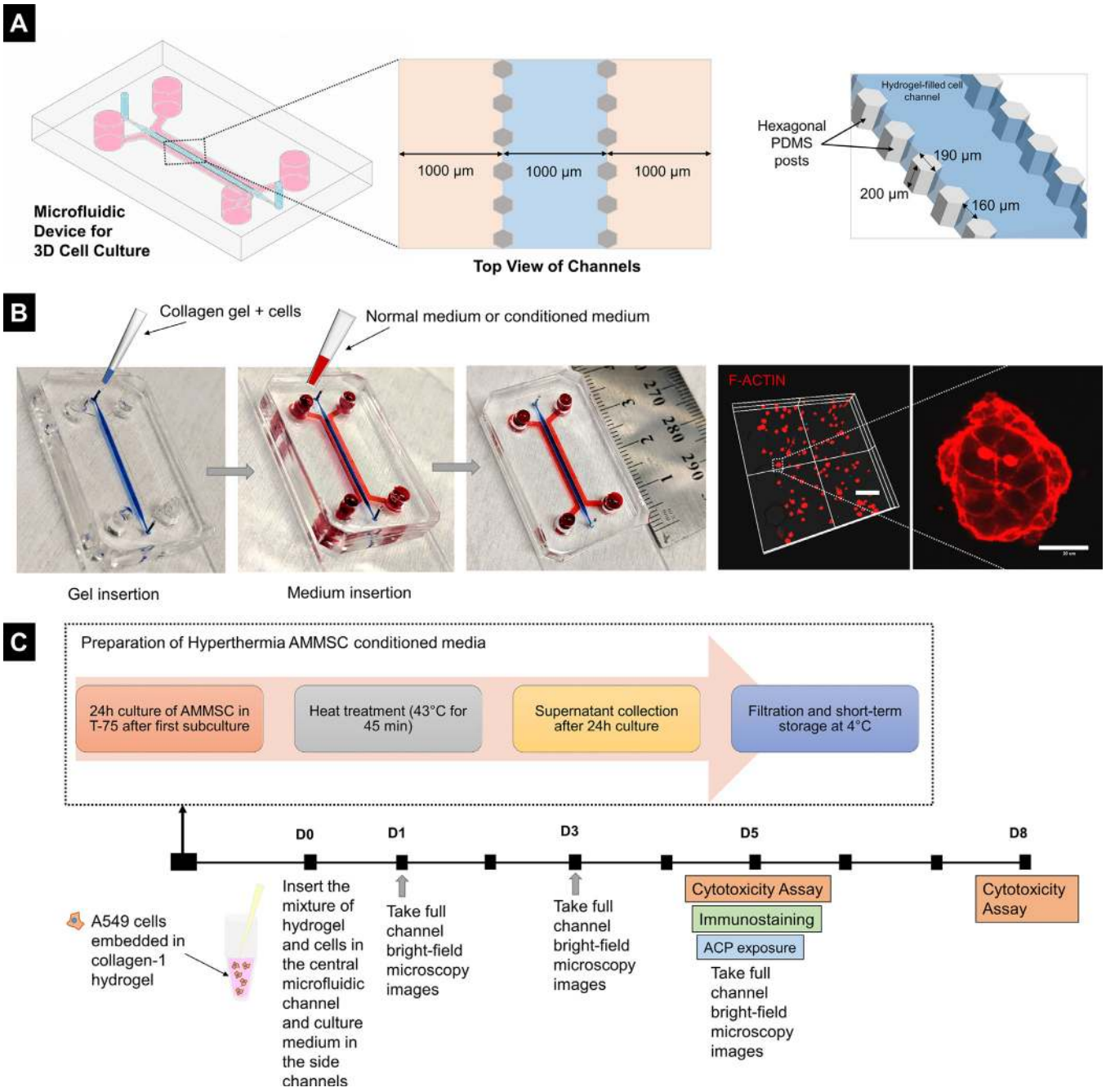

Figure 1. A 3D tumor cell culture inside a microfluidic device and experimental plan. (A) Schematic of the microfluidic device used to culture A549 lung carcinoma cells in the 3D collagen hydrogel matrix. Three channels separated by hexagonal posts along with the dimensions of each channel (top). Dimensions of hexagonal posts and gaps between posts, with hydrogel (blue) restricted in the central channel. (B) The final microfluidic device was fabricated using soft lithography, with the top layer containing channels made out of PDMS bonded to a lower layer made of a glass coverslip. The central channel was filled with a mixture of hydrogel and cells (blue) and side channels with cell culture medium (red). Photo of the final device with scale. The 3D reconstructed CLSM images of the cell-hydrogel channel showing the tumor spheroids stained for F-actin. (C) Before the main microfluidic experiment, conditioned media were prepared using human AMMSCs and heat-treated human AMMSCs for indirect co-culture experiments. ACP was added on day 5, and tumor cells were exposed for 3 days. Scale bar is 200 μm and 20 μm. CLSM, confocal laser scanning microscopy. (Color version of figure is available online).

24 h before media renewal. Previous studies have employed similar 3D microfluidic chips that are designed for developing other types of cancer models [28,29,34]. Collagen is the most abundant protein in the extracellular matrix and hence is a very suitable and established hydrogel for *in vitro* cancer modeling [35]. The confocal laser scanning microscopy images in Figure 1B show the A549 cancer spheroids inside the collagen hydrogel stained for F-actin after 5 days of cell culture in the microfluidic device. The expansion and proliferation of A549 tumor cells into tumor spheroids within the 3D space in the collagen-incorporated microfluidic channel were monitored and characterized after 5 days of culture.

Growth characterization of tumor spheroids: co-culture accelerated tumor growth

For indirect co-culture, either AMMSC-CM or heat-AMMSC-CM was added to the A549 cancer cells in the collagen matrix-incorporated microfluidic channels, and the effect of conditioning on the

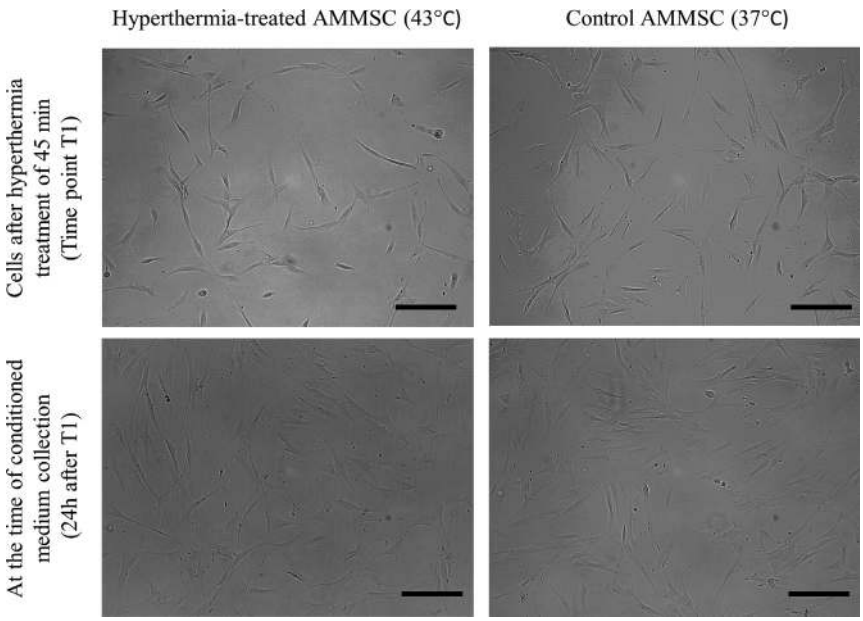

Figure 2. Hyperthermia treatment on human AMMSCs. Optical micrographs (first row) show the bright-field images of human AMMSCs before (untreated AMMSCs kept at usual 37°C) and after heat treatment at 43°C for 45 min. Images in the second row show AMMSCs in both treatment groups 24 h after the hyperthermia treatment (time point T1). Scale bar is 200 μm.

growth of cells was observed for 5 days (Figure 1C). The number of cells (AMMSCs) seeded in the T-75 flasks for both the heat-treated and untreated groups was equal (0.375×10^6 cells). The experiment timeline in Figure 1C shows that the conditioned media were collected from both groups at the same time point on the cell growth curve. The hyperthermia treatment on the human AMMSCs at 43°C for 45 min did not cause any significant changes in cell morphology, as shown in the bright-field images (Figure 2). The temperature and time duration of the hyperthermia treatment on AMMSCs were determined based on previous studies [11,36]. After the collection of conditioned media, we performed Trypan Blue assay to count live and dead cells using a hemocytometer. We found >95% of cells to be viable, although data were not saved in images. In addition, literature reports have confirmed our observation that MSCs, including AMMSCs, do not undergo serious structural damage or molecular changes during or post-hyperthermia [11,13,36]. Another study has demonstrated that after receiving heat shock pretreatment at 42°C for 1 h, bone marrow MSCs display their lowest apoptotic rate, owing to the elevated expression of heat shock proteins (HSPs) HSP70 and HSP90 inside the cells [37].

The optical micrographs (Figure 3A) revealed the transformation of tumor cells into cellular aggregates over the 5 days of cell culture in the collagen microenvironment. Previous research on 3D cancer models has reported [15,31] that after incorporation into hydrogels such as collagen or Matrigel, cancer cells tend to aggregate and form multicellular spheres/acini during proliferation. To differentiate aggregates from spheroids, we categorized cell aggregates as those having a diameter <35 μm, with tumor spheroids being larger than 35 μm [28,29]. After 1 day in culture, no significant difference was detected in the number of spheroids between the monoculture, co-culture and heat-co-culture groups (Figure 3A,B). In addition, the number of spheroids was low for all 3 groups at day 1, and no significant difference was observed in the average diameter of the tumor spheroids (Figure 3A–C). However, rapid growth was observed between day 1 and day 3 in the co-culture group compared with the monoculture group. On day 3, the number of spheroids (i.e., cell aggregates with a diameter >35 μm) was significantly higher for the co-culture (~610) and heat-co-culture groups (~435) compared with the monoculture group (~25) (Figure 3B). A similar trend could be seen in the day 3 values regarding average diameter of the spheroids, which indicated the growth-enhancing effect of indirect co-culture with AMMSC media (Figure 3C). On day 3, the co-culture and heat-co-culture groups had significant increases in average diameter ($P< 0.005$).

By day 5, the co-culture group showed a high number of spheroids (438) compared with the monoculture group (109) (Figure 3A,C). Interestingly, the number of spheroids for the co-culture group did not change after day 3 of cell culture, whereas the average diameter showed a consistent increase even after the third day (Figure 3B,C). On day 5, the average diameter for the co-culture group was 44 μm, whereas it was only 38 μm for the monoculture group, indicating a significant increase of 15.7% ($P< 0.005$). The authors have shown in an earlier study that cancer cells do not migrate to form tumor spheroids; instead, they undergo proliferation to form cellular aggregates, as confirmed by non-significant variations in the total number of cellular aggregates [22]. Therefore, it can be concluded that most of the cell aggregates in the monoculture group had a slower growth rate compared with the co-culture groups and reached a diameter of >35 μm only after 5 days of culture. Furthermore, the size distribution at day 5 clearly shows that the monoculture group had the maximum number of spheroids, with a diameter in the range of 25–40 μm. By contrast, the co-culture and heat-co-culture groups had spheroids between 35 and 60 μm and 30 and 50 μm, respectively (Figure 3D). The data for spheroids with a diameter <35 μm mainly emphasize that monocultures had a fairly equivalent number of tumor aggregates (implying that an equal number of cells were added in all groups) compared with the other 2 groups (Figure 3D), whereas Figure 3B shows less than 200 spheroids in the monoculture group. Furthermore, Figure 3D highlights the significantly high number of small aggregates (<35 μm) in the monoculture group, whereas their presence is much lower in the co-culture groups.

Previous studies have reported co-culture of cancer cells with other types of tumor stromal cells in a similar microfluidic collagen-based microenvironment [28,29]. These studies found similar growth behavior and transformation of single cancer cells into multicellular cancer spheroids. For instance, the direct co-culture of tumor stromal cells with cancer cells encapsulated in collagen inside a 7-channel microfluidic device led to enhanced growth and proliferation of cancer spheroids and increased secretion of extracellular matrix (ECM) proteins fibronectin and vimentin in 2 different studies involving colorectal and pancreatic cancer cells. The growth characterization

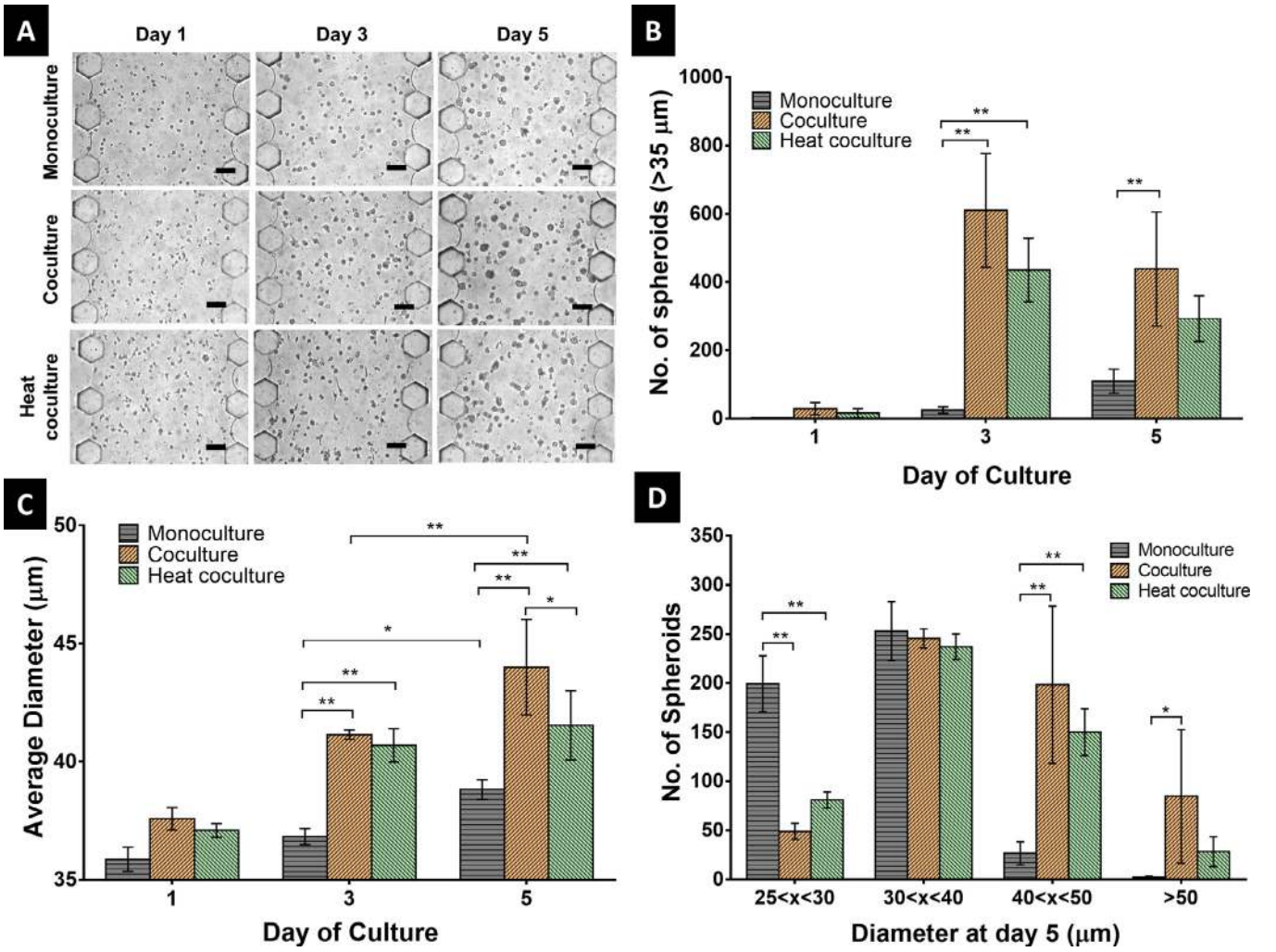

Figure 3. Growth analysis of tumor spheroids in the 3D collagen environment. (A) Optical micrographs show the growth of A549 lung carcinoma cells into tumor spheroids inside the 3D collagen matrix for all experimental groups at day 1, day 3 and day 5 of cell culture. (B) Comparison of the number of tumor spheroids (cell aggregates with diameter >35 μm) between the 3 groups from day 1 up to day 5 of cell culture. (C) Average diameter of tumor spheroids (>35 μm) plotted for day 1, day 3 and day 5 of cell culture across all 3 experimental groups. (D) Size distribution of tumor spheroids on day 5 of cell culture. Size of tumor spheroids was calculated using the formula $a = \pi r^2$ and circularity parameter of 0.8–1 using ImageJ software. Data were shown as mean ± SD of 3 independent experiments (n = 3, three different microfluidic devices in each experimental group and 20 images per microfluidic device). Two-way ANOVA, followed by Tukey's multiple comparisons test, was performed to test the statistical significance among and between groups. Scale bar is 200 μm. $^{*}P < 0.05$, $^{**}P < 0.005$. ANOVA, analysis of variance; SD, standard deviation. (Color version of figure is available online).

results for spheroids in this study indicate that the conditioned medium from AMMSC cells used for indirect co-culture of tumor spheroids had a growth-promoting effect on the A549 cells. Interestingly, these results contradict previous reports, which have shown that MSCs derived from amniotic membranes have a tumor-inhibiting effect in both *in vitro* and *in vivo* cultures [7,36,38,39]. For instance, the proliferation of 2D cultured ovarian cancer cells was found to decrease in the presence of medium conditioned by amniotic fluid-derived MSCs, as confirmed by quantitative spectrophotometry [36]. In another *in vitro* study, Magatti *et al.* [39] demonstrated that AMMSCs inhibited tumor cell proliferation in Saos2 cells by inducing cell cycle arrest at the G0/G1 phase via modulation of key cell cycle genes. In another study, AMMSCs induced apoptosis in glioma cells and significantly reduced glioma tumor size (49.5% by volume) *in vivo* [38]. The latter study was performed in *in vivo* (nude mice model) conditions, in contrast to our *in vitro* study, which used a 3D microfluidic tumor model that did not have important *in vivo* parameters such as vasculature and essential tumor stromal elements. Yet there is one study in the literature that is in agreement with the outcomes of our study; however, it was conducted in 2D cultures as well as *in vivo*, though the *in vivo* results were inconclusive [40]. Another study has shown that AMMSC-CM has no effect on A549 cell proliferation in 2D cultures [41]. Altogether, the paradoxical results in the literature necessitate further research with superior pre-clinical *in vitro* models that can better mimic the *in vivo* human tumor environment—for instance, 3D tumor spheroids with vasculature as well as other tumor stromal cell types.

The hyperthermia-conditioned AMMSC medium had a growth-stimulating effect on A549 spheroids during the first 3 days of culture. However, by day 5 there was relatively less growth in the tumor spheroids (Figure 3C). There was only a 10% increase in the size of spheroids in the heat-treated co-culture group from day 1 to day 5. By contrast, it was 18.9% in the co-culture group, implying a significant reduction of 8.9% in the diameter of spheroids belonging to the heat-co-culture group ($P < 0.05$). The significantly less growth in this group, due to the heat-AMMSC-CM (10%), was similar to that of the monoculture group, where the average diameter increase was just 8%. In addition, there was no significant difference ($P > 0.05$) in the number of spheroids between the monoculture (109) and heat-co-culture groups (293) on day 5 (Figure 3B). Previous studies of hyperthermia effects on various cancer cells were tested using 2D culture

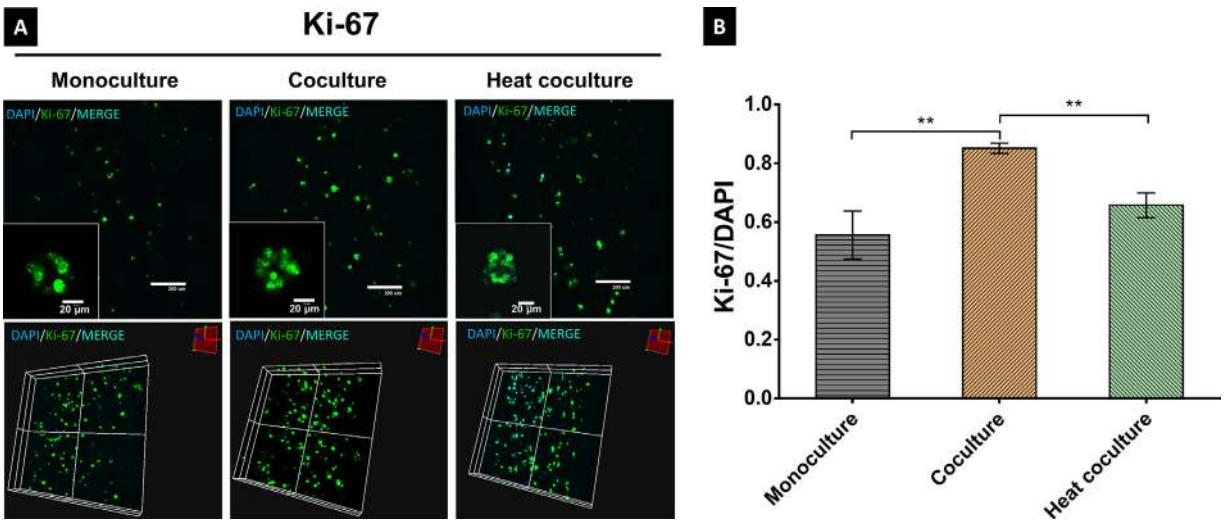

Figure 4. Immunocytochemistry assay. Immunofluorescence was performed on all groups to determine tumor cell proliferation on day 5 of culture. (A) CLSM images show the expression of cell proliferation marker Ki-67 in the tumor spheroids (A549 lung carcinoma cells). Optical sections were taken at 3-μm intervals, and Z-stacks were processed together to form 3D reconstruction images, as shown in the lower panels. (B) Quantitative fluorescent intensity data of Ki-67 from the micrographs shown in (A) for the 3 groups. ImageJ software was used to calculate the fluorescent intensity of Ki-67 from the combined Z-stacks. DAPI intensity was used to normalize the K-67 intensity. Data are shown as mean ± SD of 3 independent experiments (3 different microfluidic devices per group). Student's *t*-test (unpaired) was performed to test the statistical significance among the groups. Scale bar is 200 μm and 20 μm. $^{*}P < 0.005$. CLSM, confocal laser scanning microscopy; SD, standard deviation. (Color version of figure is available online).

platforms, in which 3D cancer spheroid growth is not possible [11,36]. Similar in-depth characterization of the growth of tumor spheroids in the presence of conditioned medium was not found elsewhere for comparison. Moreover, the number of spheroids was great enough to perform comparative statistical analysis using bright-field optical microscopy images. Therefore, we did not use DAPI to count cells in each spheroid. Counting cells in each spheroid would be interesting but was beyond the scope of the current study.

Co-culture enhanced and hyperthermia diminished tumor cell proliferation

Since the number and diameter of spheroids were affected by both AMMSC-CM and heat-AMMSC-CM, we further validated this by determining the expression of a cell proliferation marker. The expression of protein Ki-67 is strictly linked with cell proliferation, and its value indicates the fraction of actively proliferating cells in a cell population [42]. The optical micrographs in Figure 4A showed the intra-nuclear expression of protein Ki-67 in the tumor spheroids. The expression of protein Ki-67 was found to be significantly higher ($P < 0.005$) in the co-culture group compared with the monoculture group after 5 days of culture (Figure 4A,B). In a previous study, AMMSCs led to a remarkable reduction in the proliferation of different cancer cell lines by blocking the G0/G1 phase of the cell cycle [39].

Furthermore, the medium conditioned with hyperthermia-treated AMMSCs led to a reduced expression of the Ki-67 protein in tumor cells (Figure 4A,B). Notably, the difference in the expression levels of Ki-67 between the monoculture and heat-co-culture groups was not significant (Figure 4A,B). This suggests that the heat treatment might have led AMMSCs to release certain biochemical factors into the culture medium, which resulted in decreased proliferation of the tumor spheroids in the heat-co-culture group, almost at a level similar to that of the tumor spheroids grown in the monoculture group. These inhibiting effects of heat-AMMSC-CM on tumor cell proliferation were found to be consistent with previous reports in the literature. Studies have shown similar inhibitory effects of the conditioned medium by heat-treated MSC cultures on various cancer cell types grown in a monolayer or 2D culture [11,36]. For instance, Cho *et al.* [36] demonstrated that the proliferation of human carcinoma cells (ovarian and breast) was significantly inhibited in the presence of media conditioned by heat-shocked adipose tissue- and amniotic fluid-derived MSCs. They discovered that this effect was caused by cytokines released by heat-shocked MSCs, condensation of the tumor cell nucleus and alterations in the messenger RNA expression of important apoptotic proteins [36].

Ki-67 was measured on day 5, and the value of Ki-67 was normalized to the DAPI intensity so that the number of cells or spheroids did not affect the comparison. On day 5, the size of the spheroids in the heat-co-culture group was larger than that seen in the monoculture group (Figure 3B), which could be due to a sudden increase in the size by day 3 itself compared with the monoculture group. However, the number of spheroids on day 5 was not significantly different between the two groups ($P > 0.05$) (Figure 3B). The diameter of spheroids in the heat-co-culture group did not increase ($P = 0.5078$) between day 3 and day 5, and neither did the number of spheroids ($P = 0.14$), whereas the diameter of spheroids in the monoculture group increased significantly ($P < 0.05$) between day 3 and day 5. We argue that this lack of upsurge in the number and average diameter of spheroids in the heat-co-culture group from day 3 to day 5 suggests a reduction in the proliferation potential of the cells, and therefore expression of proliferation marker Ki-67 was the same in both groups. It was the absence of an increase in the diameter from day 3 to day 5 that was remarkable here, not just the value of the diameter on day 5.

As discussed previously, reports in the literature have suggested that AMMSCs suppress tumor growth. However, these studies were performed using 2D culture platforms, which are now widely considered unreliable and physiologically and pathologically irrelevant. Our study with tumor spheroids inside a 3D collagen-based microenvironment is a better replica of *in vivo* tumor characteristics than conventional 2D culture models for several reasons. For example, tumor cells are distributed in a 3D microenvironment, intercellular communication in the hydrogel is not lost in the culture medium and cell-matrix interactions and tumor spheroid formation are similar to actual cancer tissues. Therefore, it would not be implausible to conclude that the contradictory results obtained in our microfluidic cancer model compared with 2D models are worth investigating further to more clearly understand the detailed mechanisms of MSC-tumor interactions (direct or indirect).

One limitation of our study is that it was mainly focused on a 1-way indirect co-culture. Here the MSC-conditioned medium was

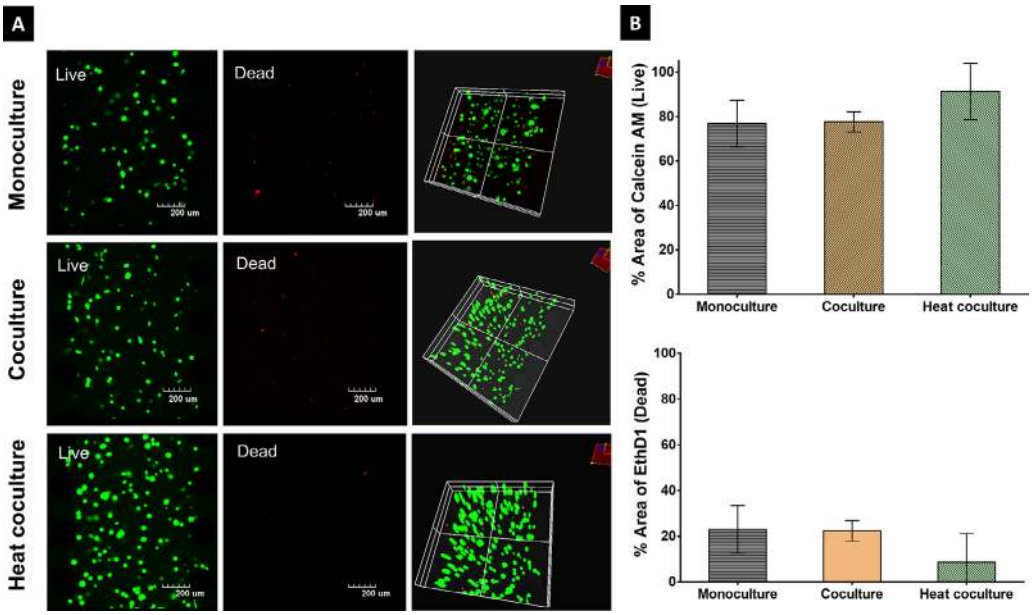

Figure 5. Cytotoxicity (live/dead) assay. (A) Cytotoxicity assay was performed on all experimental groups on day 5 of cell culture using Calcein AM (green) and EthD1 (red) fluorescent dyes. Confocal microscope images show the live cells in green and dead cells in red. The 3D reconstruction images show the entire height of the 3D hydrogel containing tumor spheroids. (B) Quantitative data from the confocal micrographs (A) were obtained using ImageJ software. Optical sections were taken at 3-μm intervals, and Z-stacks were stitched together to form 3D reconstruction images (final column) (A). Areas for both dyes were calculated and expressed as percentage area fractions [(live area or dead area)/total area]. Data are shown as mean ± SD of 3 independent experiments (3 different microfluidic devices per group). Student's *t*-test (unpaired) was performed to test the statistical significance among the groups. Scale bar is 200 μm. EthD1, Ethidium Homodimer I; SD, standard deviation. (Color version of figure is available online).

added to the tumor spheroids, whereas the MSCs were grown without any interaction—direct or indirect—with the cancer cells. Hence, in the future, we need to study tumor growth in a 2-way indirect co-culture of both aforementioned cells. In addition, a direct co-culture of both cell types inside the 3D microfluidic chip would further unravel relevant details of tumor-MSC interactions. Moreover, it would be interesting to study the effects of co-culture and hyperthermia on the expression of proteins associated with the tumor microenvironment, such as fibronectin, E-cadherin and vimentin, which could tell us about the molecular mechanism behind the results observed in the current study. Other types of cancer cells can also be tested for spheroid growth in co-culture settings. Although we have documented the effect of MSC-conditioned media on cancer cells, to uncover the mechanisms of action, a very detailed analysis of the secretome would need to be undertaken, which is beyond the scope of this study.

Influence of AMMSC co-culture on tumor cell viability

To ascertain whether the indirect co-culture with AMMSCs had any effect on cancer cell viability, a cytotoxicity assay was performed after 5 days of cell culture. The optical micrographs and 3D reconstruction images demonstrated that there were very few dead cells in all culture groups at day 5 (Figure 5A). The quantitative analysis of the micrographs also confirmed that there was no significant difference in cell viability between the monoculture and co-culture groups after this period (Figure 5B), indicating that the indirect co-culture of AMMSCs with the A549 tumor spheroids did not induce tumor cell death. One study that tested human lung-derived MSC-conditioned medium against a malignant pleural mesothelioma cell line showed cell viability reducing from 100% to 30% and 20% after 48 h and 72 h, respectively [21]. However, the AMMSC-CM results obtained in our 3D microfluidic study did not diminish cancer cell viability, but rather enhanced cell proliferation. There are studies in the literature conducted in 2D cancer culture that have shown similar effects of MSC-conditioned medium on cell viability. For instance, although one study found that the conditioned medium from human umbilical cord MSCs significantly enhanced viability of glioblastoma cells by more than 60% in 6 days [43], a similar study showed that MSCs obtained from the same source did not alter the viability of A549 lung cancer cells [44].

The heat-co-culture experiments displayed similar cell viability compared with the other groups. This could also indicate that, for hyperthermia to have considerably higher cytotoxic effects on cancer cells in the co-culture, heat treatment might need to be applied directly to co-cultured tumor spheroids and not indirectly using conditioned medium [9,10]. However, this result also verified that the inhibition of cell proliferation in the heat-co-culture (Figure 4B) was not mediated by cell death. Nevertheless, we question whether there could be a synergistic effect of heat treatment and anti-cancer drugs in suppressing tumor growth.

The contradictory results with regard to cell viability in our study compared with the literature could be due to the different MSC sources used, cancer types and/or cell culture platforms [20]. Monolayer cell culture platforms are essentially incomplete and lack the essential components of the tumor microenvironment, such as ECM, spatiotemporal distribution of cells and biomolecules, realistic cell-cell distances, cell morphology and microvasculature [15,45]. Microfluidic platforms incorporating ECM components that organize cells in 3D space hold promise since they include all these parameters and can therefore help achieve clinically relevant results in terms of understanding cancer cell biology and developing new cancer treatments [45].

Differential ACP sensitivity of tumor spheroids induced by AMMSC-conditioned medium

To test the 3D tumor microfluidic model against an anti-cancer agent, ACP P1 was chosen. ACPs have been gaining attention as promising anti-cancer drug candidates. They have the potential to overcome the challenges faced by conventional anti-cancer drugs, such as chemotherapeutic resistance and lack of specificity [46]. Our peptide,

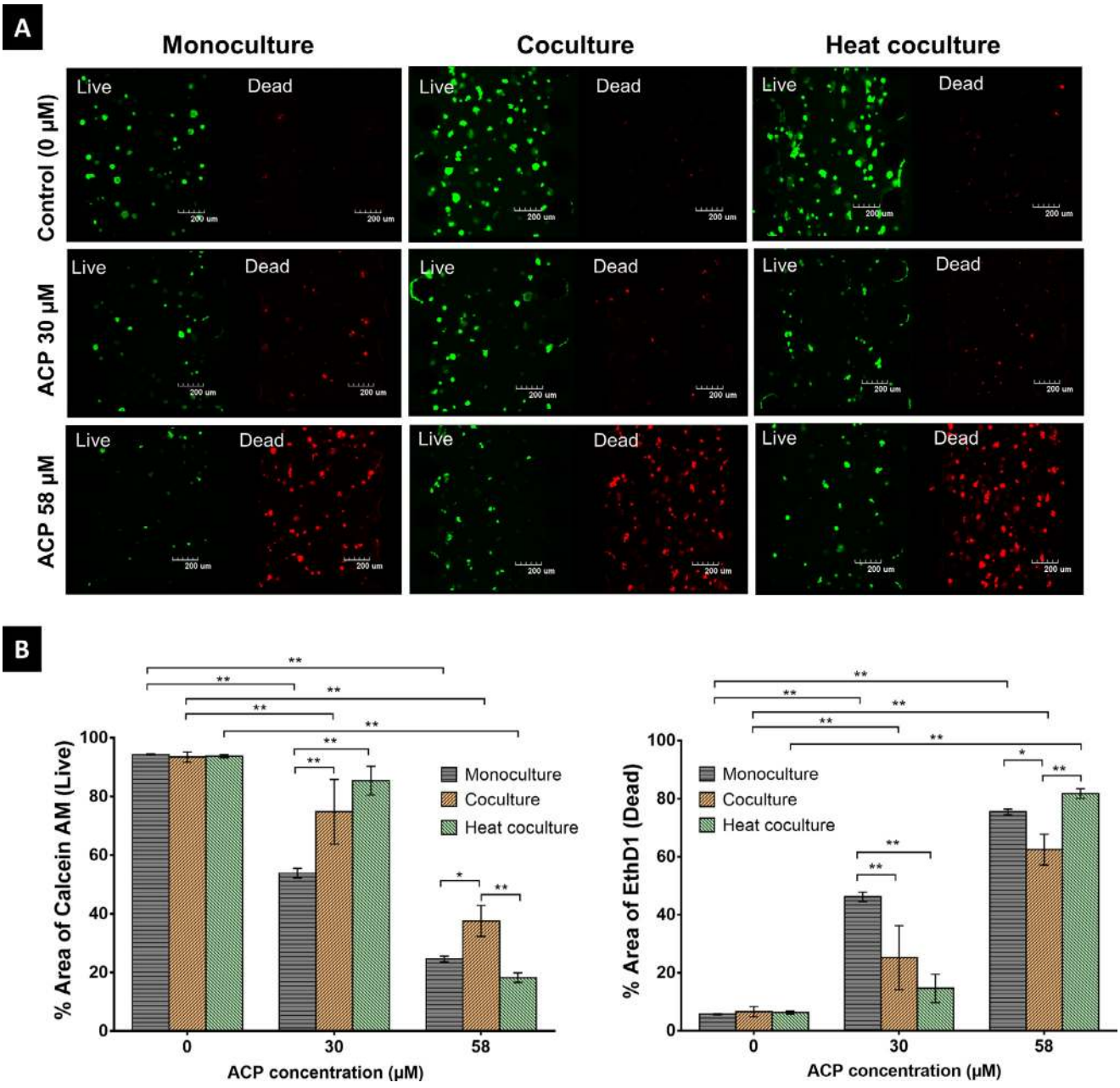

Figure 6. Screening of ACP P1 and cytotoxicity assay. (A) Cytotoxicity assay was performed on all experimental groups after 3-day (72 h) exposure to 2 different concentrations of ACP P1 using Calcein AM (live, green) and EthD1 (red, dead) fluorescent dyes. (B) Quantitative data from the micrographs were obtained using ImageJ software. Optical sections were taken at 3-μm intervals, and Z-stacks were stitched together to obtain 3D reconstruction images. Areas for both dyes were calculated and expressed as percentage area fractions [(live area or dead area)/total area]. Data are shown as mean ± SD of 3 independent experiments (3 different microfluidic devices per group). Two-way ANOVA, followed by Tukey's multiple comparisons test, was performed to test the statistical significance among and between groups. Scale bar is 200 μm. *$P<$ 0.05, **$P<$ 0.005. ANOVA, analysis of variance; EthD1, Ethidium Homodimer I; SD, standard deviation. (Color version of figure is available online).

P1, was designed to be highly positively charged, displaying high specificity toward cancer cells compared with healthy cells [22,30]. All 3 experimental groups were exposed to this ACP at 2 different concentrations (30 μM and 58 μM) for 3 days of culture, followed by cell viability determination. Screening of only the clinically relevant concentrations was performed on the chip to demonstrate the anticancer potential of the peptide on the microfluidic 3D cultures, earlier tested by the authors' group in 2D models [30]. The concept of clinically relevant concentrations has been explained in detail in the authors' previous work (i.e., 3D microfluidic model) [22]. We observed no significant difference in cell viability among the 3 groups that were not exposed to the peptide (control, 0 μM). However, there was a significant reduction ($P<$ 0.005) in cell viability in all 3 experimental groups as the peptide dose was increased from 0 μM to 30 μM and, finally, 58 μM (Figure 6A,B). The confocal micrographs showed both live (green) and dead (red) cells in the tumor spheroids, which were distributed throughout the 3D microenvironment (Figure 6A). Interestingly, the percentage of living or dead cells varied significantly among the 3 groups at different peptide concentrations. At 30 μM, the highest viability was seen for the co-culture and heat-co-culture groups compared with the monoculture group. The co-culture group showed 75% viability, and the heat-co-culture group displayed 85% viability, which was significantly different ($P<$ 0.005) compared with the monoculture group (54%) (Figure 6A,B). Using 58-

μM ACP, the difference in viable cells between the monoculture group (24%) and co-culture group (37%) was lower but still significant ($P< 0.05$). However, the most noteworthy reduction was observed in the heat-co-culture group, where cell viability was found to be only 18%, which was significantly lower than the co-culture group ($P< 0.005$) (Figure 6A,B).

The differences in peptide-driven cell mortality among the monoculture, co-culture and heat-co-culture groups are quite remarkable, mainly due to the fact that the peptide we used has a membranolytic mechanism of inducing cell damage or death [30] and therefore should not ideally differentiate between different culture conditions. These differences could be due to this particular peptide affecting cells in ways other than the mechanisms mentioned earlier, as was shown in the authors' previous work [22]. We had observed that the spheroid-forming capability as well as the proliferation ability of the tumor cells was significantly reduced after exposure to this peptide for 5 days [22]. Thus here, the highly proliferating tumor cells in the co-culture group were not affected by the aforementioned property of the ACP during the 72 h of peptide exposure. However, the heat-co-culture group, having cells with relatively lower proliferating capability (Figure 4A,B), was affected to a greater extent by the cell-damaging and proliferation-reducing capabilities of the peptide at higher peptide concentration (58 μM). In other words, the heat-AMMSC-CM could have sensitized the cancer cells over 5 five days of culture; therefore, the number of available peptides was high enough to damage a large percentage of cancer cells in the spheroids. The cell viability trend among the 3 experimental groups at this peptide concentration was in agreement with the proliferation data, where the Ki-67 expression of the heat-co-culture group was similar to that of the monoculture group (Figure 4B). Previous studies in the literature have also shown this synergistic anti-cancer effect of hyperthermia-treated MSCs (bone marrow) and anti-cancer drugs [9,11,36]. For example, a combinatorial treatment using DNA-associated anti-cancer drugs (5 μg/mL 5-fluorouracil, 20 μM azacitidine, 40 μM genistein and 100 μM cisplatin) and the conditioned medium of heat-treated MSCs resulted in heightened inhibition of tumor cell growth, whereas the no-heat MSC medium had little or no influence [11].

There is a large amount of literature showing that amniotic MSCs exert anti-tumor effects against cancer cells, as reviewed by Kang *et al.* [7]. However, one study has shown that amniotic MSCs do not affect the proliferation of A549 cells in monolayer (2D) cultures, although this study did not identify any of the bioactive factors responsible for this behavior [41]. Additionally, this study found that the conditioned medium inhibited tumor proliferation for other cancer cell types, and it included a group of secreted factors that could be responsible for this. Cell-free conditioned media derived from MSCs can be enriched in growth factors, exosomes, cytokines and chemokines [47]. Even though the results obtained in our study showed that the AMMSC-CM has a pro-tumorigenic tendency, despite this difference, few studies have investigated the anti-tumor effects of these cells in 3D culture. Therefore, to help elucidate the results obtained in our study, we evaluated possible soluble factors secreted by human AMMSCs and their function by studying the published data.

Various cytokines, such as plasminogen activator inhibitor 1 (PAI-1), metallopeptidase inhibitor 1 (TIMP-1), granulocyte colony-stimulating factor and periostin, have been found in significantly high concentrations in AMMSC-CM [40,48]. PAI-1 has been known to inhibit spontaneous apoptosis in cancer cells via multiple mechanisms [49]. Furthermore, a recent study has shown that its inhibition might result in improved chemotherapeutic effects in non-small cell lung carcinoma cells [50]. Activation of the PI3K/AKT pathway (an intracellular signaling pathway) [48] due to PAI-1 also contributes to the development of tumors and resistance to anti-cancer therapies [51] and is currently a therapeutic target for lung cancer treatments [52]. In addition, TIMP-1 is known for its anti-apoptotic role via its interaction with B-cell lymphoma 2 (Bcl-2) in lung cancer cells [53]. Thus, it could be speculated that the cytokines released by human AMMSCs, such as PAI-1 and TIMP-1, could have accelerated the tumor spheroid growth in our 3D microfluidic culture by activating the PI3K/AKT pathway [52].

Another study that delved deeper into the secretome of human AMMSCs found that around 131 genes were upregulated by more than 2-fold in AMMSC-CM compared with fibroblast CM [54]. Using cytokine profiling, the study authors found that numerous soluble factors were secreted by human AMMSCs, including basic fibroblast growth factor (bFGF), IL-6 (interleukin-6), insulinlike growth factor 1 and vascular endothelial growth factor (VEGF). This study also demonstrated that pro-survival signaling pathways such as ERK1/2 MAPK were activated in cells because of the presence of these cytokines in the human AMMSC-CM. The ERK1/2 MAPK pathway is known to be highly activated in aggressive lung cancer cells as well [55]. The bFGF released by human AMMSCs is an anti-apoptotic factor and stimulates the growth of lung tumor cells by intracrine mechanisms [56]. Studies have also demonstrated that the exosomes secreted by MSCs could encourage cancer cells to release VEGF, which has a tendency to promote tumor growth by activating the ERK1/2 pathway [57,58]. Hence, we theorize that the possible secretion of cytokines such as PAI-1, TIMP-1, bFGF, VEGF and IL-6 by AMMSCs in the conditioned medium could explain the pro-tumorigenic results obtained in our study. Further experiments are required to prove this hypothesis, with the main aim of delving deeper into the constituents of the human AMMSC secretome, especially those that are directly responsible for the accelerated growth of lung tumor spheroids.

Pre-conditioning the AMMSCs to 43°C hyperthermia could have led to variations in the paracrine profile of the AMMSCs. As the study by Cho *et al.* [36] showed, the conditioned medium of amniotic MSCs significantly increased cytoskeleton breakdown of the human ovarian cancer cell line SK-OV-3, with prominent nuclear condensation and increased apoptotic cell death. Another study by Park *et al.* [11] showed that heat treatment of bone marrow MSCs at 43°C resulted in increased secretion of class II transactivator (master regulator of major histocompatibility complex), CD80, IL-16 and tumor necrosis factor α (a well-known anti-neoplastic factor) into the conditioned medium. Also, the combination of chemotherapeutic drugs and heat-treated conditioned medium could lead to enhanced tumor cell mortality via apoptosis, which could involve upregulation of tumor necrosis factor R (a key player in transmitting death signals during chemotherapy) and downregulation of multidrug resistance protein 1 and anti-apoptotic protein Bfl-1, which play a key role in anti-cancer drug resistance [11]. Moreover, major histocompatibility complex class II molecules have recently been noted to play an important role in anti-tumor immunity [59]. Both of these studies concluded that hyperthermia treatment led to the transition of the pro-tumorigenic environment found in normal MSC-conditioned medium to the anti-tumorigenic environment found in heat-treated MSC-conditioned medium. Similar paracrine factors could have been released in the human AMMSC-conditioned medium in our study, which could have possibly induced cell apoptotic mechanisms in the lung tumor spheroids. Future investigation into the soluble factors released by human AMMSCs after heat treatment would shed more light on the anti-cancer mechanisms.

Conclusions

We have shown that a simple microfluidic platform is a suitable and physiologically relevant platform with which to form A549 tumor spheroids in a 3D collagen-based hydrogel. The microenvironment created allowed a number of variations to the experimental protocol that deciphered the synergistic role played by both MSCs and an ACP in reducing cancer cell growth. The indirect co-culture of A549 cells with AMMSCs using the AMMSC-CM considerably and rapidly increased A549 tumor spheroid size and proliferation

compared with the monoculture group. The hyperthermia treatment performed on AMMSCs proved to be effective against tumor spheroid growth, especially in combination with the ACP P1. However, neither AMMSC-CM nor heat-AMMSC-CM alone led to cancer cell death after 5 days of cell culture. Our results clearly contradict what has been observed so far in relation to AMMSCs and their impact on cancer cells when studied using 2D models [7]. Therefore, the therapeutic potential of AMMSCs in cancer research remains undetermined and necessitates further research involving physiologically relevant preclinical *in vitro* models. The results obtained in this study suggest that MSCs, heat treatment and ACPs play a significant role in inhibiting tumor growth when used in combination with a 3D tumor spheroid model.

Declaration of Competing Interest

The authors have no commercial, proprietary or financial interest in the products or companies described in this article.

Funding

This work was funded by both the Swinburne University of Technology Postgraduate Research Award, Australia, and the Nano Mission Project, Department of Science and Technology, Government of India (project reference no. SR/NM/NT- 1095/2016). ND was supported by Swinburne University of Technology Postgraduate Research Award and Ministry of Human Resource Development, Government of India, fellowships.

Author Contributions

Conception and design of the study: ND, HS and PK. Acquisition of data: ND. Analysis and interpretation of data: ND, SNR and PK. Drafting or revising the manuscript: ND. All authors have revised and approved the final article.

Acknowledgments

The authors thank Dr Rohan Shah, Prof Richard Manasseh and Dr Tomas Katkus at Swinburne University of Technology, Australia, for providing the A549 lung carcinoma cells, the human amniotic membrane-derived mesenchymal stem cells, and for technical assistance, respectively. The authors thank Dr Chandra S. Sharma and Mr Suresh Mamidi for photolithography training and technical support at Indian Institute of Technology Hyderabad, India. This research work was accomplished in part at both the Biointerface Engineering Hub at Swinburne University of Technology, Australia, and the Melbourne Centre for Nanofabrication in the Victorian Node of the Australian National Fabrication Facility.

Data Availability

The experimental data required to reproduce the findings from this study are present in this article, and additional data will be made available to interested investigators upon request.

References

[1] Dominici M, Le Blanc K, Mueller I, Slaper-Cortenbach I, Marini FC, Krause DS, et al. Minimal criteria for defining multipotent mesenchymal stromal cells. The International Society for Cellular Therapy position statement. Cytotherapy 2006;8:315–7.
[2] Reagan MR, Kaplan DL. Concise review: Mesenchymal stem cell tumor-homing: Detection methods in disease model systems. Stem Cells 2011;29:920–7.
[3] Melzer C, Yang Y, Hass R. Interaction of MSC with tumor cells. Cell Commun Signal 2016;14:1–12.
[4] Christodoulou I, Goulielmaki M, Devetzi M, Panagiotidis M, Koliakos G, Zoumpourlis V. Mesenchymal stem cells in preclinical cancer cytotherapy: a systematic review. Stem Cell Res Ther 2018;9:336.
[5] Shah K. Mesenchymal stem cells engineered for cancer therapy. Adv Drug Deliv Rev 2012;64:739–48.
[6] Sage EK, Thakrar RM, Janes SM. Genetically modified mesenchymal stromal cells in cancer therapy. Cytotherapy 2016;18:1435–45.
[7] Kang N-H, Hwang K-A, Kim SU, Kim Y-B, Hyun S-H, Jeung E-B, et al. Potential antitumor therapeutic strategies of human amniotic membrane and amniotic fluid-derived stem cells. Cancer Gene Ther 2012;19:517–22.
[8] Schmidt F, Efferth T. Tumor Heterogeneity, Single-Cell Sequencing, and Drug Resistance. Pharmaceuticals (Basel) 2016;9:33.
[9] Yagawa Y, Tanigawa K, Kobayashi Y, Yamamoto M. Cancer immunity and therapy using hyperthermia with immunotherapy, radiotherapy, chemotherapy, and surgery. J Cancer Metastasis Treat 2017;3:218.
[10] Elliott RS, Storm FK, Morton DL. Normal tissue and solid tumor effects of hyperthermia in animal models and clinical trials. Cancer Res 1979;39:2245–51.
[11] Park H, Cho J-A, Kim S-K, Kim J-H, Lee S-H. Hyperthermia on mesenchymal stem cells (MSCs) can sensitize tumor cells to undergo cell death. Int J Hyperth 2008;24:638–48.
[12] Alekseenko LL, Shilina MA, Lyublinskaya OG, Kornienko JS, Anatskaya OV, Vinogradov AE, et al. Quiescent human mesenchymal stem cells are more resistant to heat stress than cycling cells. Stem Cells Int 2018;2018:3753547.
[13] Hesami S, Mohammadi M, Rezaee MA, Jalili A, Rahmani MR. The effects of hyperthermia on the immunomodulatory properties of human umbilical cord vein mesenchymal stem cells (MSCs). Int J Hyperthermia 2017;33:705–12.
[14] Sontheimer-Phelps A, Hassell BA, Ingber DE, John Paulson HA. Modelling cancer in microfluidic human organs-on-chips. Nat Rev Cancer 2019;19:65–81.
[15] Dhiman N, Kingshott P, Sumer H, Sharma CS, Rath SN. On-chip anticancer drug screening—recent progress in microfluidic platforms to address challenges in chemotherapy. Biosens Bioelectron 2019;137:236–54.
[16] Valente KP, Khetani S, Kolahchi AR, Sanati-Nezhad A, Suleman A, Akbari M. Microfluidic technologies for anticancer drug studies. Drug Discov Today 2017;22:1654–70.
[17] Abbott RD, Kaplan DL. Strategies for improving the physiological relevance of human engineered tissues. Trends Biotechnol 2015;33:401–7.
[18] Sung KE, Beebe DJ. Microfluidic 3D models of cancer. Adv Drug Deliv Rev 2014;79:68–78.
[19] Bhatia SN, Ingber DE. Microfluidic organs-on-chips. Nat Biotechnol 2014;32:760–72.
[20] Gunawardena TNA, Rahman MT, Abdullah BJJ, Abu Kasim NH. Conditioned media derived from mesenchymal stem cell cultures: The next generation for regenerative medicine. J Tissue Eng Regen Med 2019;13:569–86.
[21] Cortes-Dericks L, Froment L, Kocher G, Schmid RA. Human lung-derived mesenchymal stem cell-conditioned medium exerts *in vitro* antitumor effects in malignant pleural mesothelioma cell lines. Stem Cell Res Ther 2016;7:25.
[22] Dhiman N, Shagaghi N, Bhave M, Sumer H, Kingshott P, Rath SN. Selective Cytotoxicity of a Novel Trp−Rich Peptide against Lung Tumor Spheroids Encapsulated inside a 3D Microfluidic Device. Adv Biosyst 2020;4:1900285.
[23] Marongiu F, Gramignoli R, Sun Q, Tahan V, Dorko K, Ellis E, et al. Current Protocols in Stem Cell Biology. Curr Protoc Stem Cell Biol 2007;12:1–11.
[24] Wang P-Y, Ding S, Sumer H, Wong RC-B, Kingshott P. Heterogeneity of mesenchymal and pluripotent stem cell populations grown on nanogrooves and nanopillars. J Mater Chem B 2017;5:7927–38.
[25] Shah RM, Eldridge DS, Palombo EA, Harding IH. Microwave-assisted formulation of solid lipid nanoparticles loaded with non-steroidal anti-inflammatory drugs. Int J Pharm 2016;515:543–54.
[26] Eswaramoorthy SD, Dhiman N, Korra G, Oranges CM, Schaefer DJ, Rath SN, et al. Isogenic-induced endothelial cells enhance osteogenic differentiation of mesenchymal stem cells on silk fibroin scaffold. Regen Med 2019;14:647–61.
[27] Schindelin J, Arganda-Carreras I, Frise E, Kaynig V, Longair M, Pietzsch T, et al. Fiji: an open-source platform for biological-image analysis. Nat Methods 2012;9:676–82.
[28] Jeong SY, Lee JH, Shin Y, Chung S, Kuh HJ. Co-culture of tumor spheroids and fibroblasts in a collagen matrix-incorporated microfluidic chip mimics reciprocal activation in solid tumor microenvironment. PLoS One 2016;11:e0159013.
[29] Lee J-H, Kim S-K, Khawar IA, Jeong S-Y, Chung S, Kuh H-J. Microfluidic co-culture of pancreatic tumor spheroids with stellate cells as a novel 3D model for investigation of stroma-mediated cell motility and drug resistance. J Exp Clin Cancer Res 2018;37:4.
[30] Shagaghi N. Development of novel antimicrobial peptides. Ph.D. Thesis, Swinburne University of Technology; 2017. p. 1–314.
[31] Wang D-D, Liu W, Chang J-J, Cheng X, Zhang X-Z, Xu H, et al. Bioengineering three-dimensional culture model of human lung cancer cells: an improved tool for screening EGFR targeted inhibitors. RSC Adv 2016;6:24083–90.
[32] Shin Y, Han S, Jeon JS, Yamamoto K, Zervantonakis IK, Sudo R, et al. Microfluidic assay for simultaneous culture of multiple cell types on surfaces or within hydrogels. Nat Protoc 2012;7:1247–59.
[33] Chung S, Sudo R, Mack PJ, Wan C-R, Vickerman V, Kamm RD. Cell migration into scaffolds under co-culture conditions in a microfluidic platform. Lab Chip 2009;9:269–75.
[34] Boussommier-Calleja A, Li R, Chen MB, Wong SC, Kamm RD. Microfluidics: a new tool for modeling cancer-immune interactions. Trends in Cancer 2016;2:6–19.
[35] Zhang X, Li L, Luo C. Gel integration for microfluidic applications. Lab Chip 2016;16:1757–76.

[36] Cho JA, Park H, Kim HK, Lim EH, Seo SW, Choi JS, et al. Hyperthermia-treated mesenchymal stem cells exert antitumor effects on human carcinoma cell line. Cancer 2009;115:311–23.
[37] Wang Q, Li X, Wang Q, Xie J, Xie C, Fu X. Heat shock pretreatment improves mesenchymal stem cell viability by heat shock proteins and autophagy to prevent cisplatin-induced granulosa cell apoptosis. Stem Cell Res Ther 2019;10:348.
[38] Jiao H, Guan F, Yang B, Li J, Song L, Hu X, et al. Human amniotic membrane derived-mesenchymal stem cells induce C6 glioma apoptosis *in vivo* through the Bcl-2/caspase pathways. Mol Biol Rep 2012;39:467–73.
[39] Magatti M, Munari S, Vertua E, Parolini O. Amniotic membrane-derived cells inhibit proliferation of cancer cell lines by inducing cell cycle arrest. J Cell Mol Med 2012;16:2208–18.
[40] Meng MY, Li L, Wang WJ, Liu FF, Song J, Yang SL, et al. Assessment of tumor promoting effects of amniotic and umbilical cord mesenchymal stem cells *in vitro* and *in vivo*. J Cancer Res Clin Oncol 2019;145:1133–46.
[41] Paiboon N, Kamprom W, Manochantr S, Tantrawatpan C, Tantikanlayaporn D, Roytrakul S, et al. Gestational Tissue-Derived Human Mesenchymal Stem Cells Use Distinct Combinations of Bioactive Molecules to Suppress the Proliferation of Human Hepatoblastoma and Colorectal Cancer Cells. Stem Cells Int 2019;2019:9748795.
[42] Scholzen T, Gerdes J. The Ki-67 protein: from the known and the unknown. J Cell Physiol 2000;182:311–22.
[43] Vieira de Castro J, Gomes ED, Granja S, Anjo SI, Baltazar F, Manadas B, et al. Impact of mesenchymal stem cells' secretome on glioblastoma pathophysiology. J Transl Med 2017;15:1–14.
[44] Hendijani F, Javanmard SH, Rafiee L, Sadeghi-Aliabadi H. Effect of human Wharton's jelly mesenchymal stem cell secretome on proliferation, apoptosis and drug resistance of lung cancer cells. Res Pharm Sci 2015;10:134–42.
[45] Huh D, Hamilton GA, Ingber DE. From 3D cell culture to organs-on-chips. Trends Cell Biol 2011;21:745–54.
[46] Nyström L, Malmsten M. Membrane interactions and cell selectivity of amphiphilic anticancer peptides. Curr Opin Colloid Interface Sci 2018;38:1–17.
[47] Wang Y, Long W, Cao Y, Li J, You L, Fan Y. Mesenchymal stem cell-derived secretomes for therapeutic potential of premature infant diseases. Biosci Rep 2020;40: BSR20200241.
[48] Li JY, Ren KK, Zhang WJ, Xiao L, Wu HY, Liu QY, et al. Human amniotic mesenchymal stem cells and their paracrine factors promote wound healing by inhibiting heat stress-induced skin cell apoptosis and enhancing their proliferation through activating PI3K/AKT signaling pathway. Stem Cell Res Ther 2019;10:1–17.
[49] Placencio VR, DeClerck YA. Plasminogen Activator Inhibitor-1 in Cancer: Rationale and Insight for Future Therapeutic Testing. Cancer Res 2015;75: 2969–74.
[50] Masuda T, Nakashima T, Namba M, Yamaguchi K, Sakamoto S, Horimasu Y, et al. Inhibition of PAI−1 limits chemotherapy resistance in lung cancer through suppressing myofibroblast characteristics of cancer−associated fibroblasts. J Cell Mol Med 2019;23:2984–94.
[51] Yang J, Nie J, Ma X, Wei Y, Peng Y, Wei X. Targeting PI3K in cancer: mechanisms and advances in clinical trials. Mol Cancer 2019;18:1–28.
[52] Cheng H, Shcherba M, Pendurti G, Liang Y, Piperdi B, Perez-Soler R. Targeting the PI3K/AKT/mTOR pathway: potential for lung cancer treatment. Lung Cancer Manag 2014;3:67–75.
[53] Nalluri S, Ghoshal-Gupta S, Kutiyanawalla A, Gayatri S, Lee BR, Jiwani S, et al. TIMP-1 Inhibits Apoptosis in Lung Adenocarcinoma Cells via Interaction with Bcl-2. PLoS One 2015;10:e0137673.
[54] Danieli P, Malpasso G, Ciuffreda MC, Cervio E, Calvillo L, Copes F, et al. Conditioned Medium From Human Amniotic Mesenchymal Stromal Cells Limits Infarct Size and Enhances Angiogenesis. Stem Cells Transl Med 2015;4:448–58.
[55] Vicent S, López-Picazo JM, Toledo G, Lozano MD, Torre W, Garcia-Corchón C, et al. ERK1/2 is activated in non-small-cell lung cancer and associated with advanced tumours. Br J Cancer 2004;90:1047–52.
[56] Kuhn H, Köpff C, Konrad J, Riedel A, Gessner C, Wirtz H. Influence of basic fibroblast growth factor on the proliferation of non-small cell lung cancer cell lines. Lung Cancer 2004;44:167–74.
[57] Zhu W, Huang L, Li Y, Zhang X, Gu J, Yan Y, et al. Exosomes derived from human bone marrow mesenchymal stem cells promote tumor growth *in vivo*. Cancer Lett 2012;315:28–37.
[58] König J, Weiss G, Rossi D, Wankhammer K, Reinisch A, Kinzer M, et al. Placental Mesenchymal Stromal Cells Derived from Blood Vessels or Avascular Tissues: What Is the Better Choice to Support Endothelial Cell Function? Stem Cells Dev 2015;24:115–31.
[59] Axelrod ML, Cook RS, Johnson DB, Balko JM. Biological Consequences of MHC-II Expression by Tumor Cells in Cancer. Clin Cancer Res 2019;25:2392–402.